Hindawi Publishing Corporation
International Journal of Photoenergy
Volume 2014, Article ID 602692, 8 pages
http://dx.doi.org/10.1155/2014/602692

Research Article

TiO_2 Nanotube Arrays Composite Film as Photoanode for High-Efficiency Dye-Sensitized Solar Cell

Jinghua Hu,[1,2,3] Li Zhao,[1,2] Yingping Yang,[3] Hong Liao,[3] Shimin Wang,[1,2] Xiaodong Sun,[3] Jiejie Cheng,[3] and Binghai Dong[1,2]

[1] *Hubei Collaborative Innovation Center for Advanced Organic Chemical Materials, Wuhan 430062, China*
[2] *Ministry of Education Key Laboratory for the Green Preparation and Application of Functional Materials, Faculty of Materials Science and Engineering, Hubei University, Wuhan 430062, China*
[3] *School of Science, Wuhan University of Technology, Wuhan 430070, China*

Correspondence should be addressed to Li Zhao; zhaoli7376@163.com, Yingping Yang; y.p.yang@126.com and Shimin Wang; shiminwang@126.com

Received 7 April 2014; Revised 9 May 2014; Accepted 12 May 2014; Published 25 May 2014

Academic Editor: Wei Xiao

A double-layered photoanode made of hierarchical TiO_2 nanotube arrays (TNT-arrays) as the overlayer and commercial-grade TiO_2 nanoparticles (P25) as the underlayer is designed for dye-sensitized solar cells (DSSCs). Crystallized free-standing TNT-arrays films are prepared by two-step anodization process. For photovoltaic applications, DSSCs based on double-layered photoanodes produce a remarkably enhanced power conversion efficiency (PCE) of up to 6.32% compared with the DSSCs solely composed of TNT-arrays (5.18%) or nanoparticles (3.65%) with a similar thickness (24 μm) at a constant irradiation of 100 mW cm^{-2}. This is mainly attributed to the fast charge transport paths and superior light-scattering ability of TNT-arrays overlayer and good electronic contact with F-doped tin oxide (FTO) glass provided from P25 nanoparticles as a bonding layer.

1. Introduction

Currently, dye-sensitized solar cells (DSSCs) have attracted considerable attention as a potential alternative to conventional silicon-related solar cells owing to the high efficiency and low cost since 1991 [1]. Their overall conversion efficiencies have reached 11.2%, which was still low as compared to that of 13–25% usually reparted in the silicon-based solar cells [2]. Nanocrystalline TiO_2 photoelectrode, as one of the major components of DSSCs, is critical for the photovoltaic performance. It is well known that the DSSCs efficiency is strongly dependent on a dynamic competition between the electron transportation in TiO_2 and the interfacial charge recombination. So much effort has been made up to now on the photoanode to facilitate electron transport and retard electron recombination.

To satisfy these requirements, one-dimensional (1D) TiO_2 materials, such as nanowire [3], nanorods [4], nanofiber [5], and nanotube [6], have been successively synthesized and applied on the DSSCs. From all morphological forms of titanium dioxide for solar energy conversion, TiO_2 nanotube arrays (TNT-arrays) appear highly ordered and vertically aligned, offering electron transport properties comparable to nanoparticles. It not only exhibits few grain boundaries but also provides direct pathways for electron transportation, leading to the suppressed electron-hole recombination [7]. TNT-arrays have been fabricated by using various methods, such as sol-gel [8, 9], hydrothermal [10, 11] and chemical vapor deposition [12], and electrochemical anodization [13–16]. Electrochemical anodization has been recognized as more convenient and simpler approach to produce integrative vertically and highly ordered TNT-arrays with controllable structural morphologies [17]. However, the performance of DSSCs based TNT-arrays on Ti substrate is restricted due to the presence of opaque Ti substrate. TNT-arrays/Ti-based DSSCs required back-side illumination [18, 19] which is not an optimal approach for increasing the power conversion efficiency. Hence, the fabrication of TNT-arrays on a transparent conductive substrate for front-side illuminated DSSCs is desired and will be expected to improve photovoltaic

performance [20]. Transparent TNT-arrays/FTO glass was prepared via an anodic oxidation of titanium thin film that was sputtered onto FTO conductive glass [21], which involves the sputtering of Ti films onto FTO glass, thus leading to a high fabrication cost. Hyeoká Park and GuáKang transferred and adhered TNT-arrays onto the FTO glass using Ti isopropoxide solution as a paste [22]; however, the TNT-arrays/FTO has a very small area (0.03–0.15 cm^2) owing to the structural destruction during one step annealing. Hence, a simple process of fabricating large-scale TNT-arrays film on FTO glass is very desirable.

Herein, we fabricated a novel double-layered TiO_2 photoanode consisting of hierarchical TNT-arrays and TiO_2 nanoparticle on a FTO glass substrate. Specially, the overlayer consisting of TNT-arrays plays a dual role for both stronger light-scattering capability and fast electron transport paths, and the underlayer made of TiO_2 nanoparticles serves as a bonding layer, which offers good contact between TNT-arrays and FTO glass. As a result, the photoelectronic conversion efficiency (PCE) of 6.32% was achieved in double-layered composite film. The performance improvement is almost attributed to the stronger light-scattering capability and fast electron paths of TNT-arrays films, resulting in decreased recombination of the electron-hole. Meanwhile, it is related to the good electronic contact between TiO_2 film and the F-doped tin oxide (FTO) glass.

2. Experiment

2.1. Preparation of the TNT-Arrays/Ti Foils Substrate. TNT-arrays films were prepared by anodization of Ti foils (99.7%, 0.25 um, Aldrich) in an NH_4F/ethylene glycol electrolyte solution by using a DC power source (PPS-1206, Motech) at room temperature, while a Pt foil was used as the counter electrode. The Ti foils were first physically polished, then degreased by sonication in acetone, ethanol, and DI water. Anodization was carried out in an ethylene glycol based on electrolyte containing NH_4F (0.5 wt%) and deionized water (2 vol%) under a constant voltage of 40 V. After the anodic oxidation, the Ti foil with the TNT-arrays grown on one side of its surfaces was thoroughly washed with a large amount of DI water and ethanol.

2.2. Preparation of the P25/TNT-Arrays/FTO Glass Photoanode. In order to achieve free-standing TNT-arrays films, the grown TNT-arrays were detached from the metallic Ti substrate as described in the following. The as-anodized TNT-arrays films were annealed at 450°C for 30 min to crystallize and then reanodized in the same electrolyte at corresponding potential for 3 h to form an amorphous TiO_2 layer between the crystallized TNT-arrays and the Ti foil. Finally, the resulting film was soaked in an H_2O_2 solution (35.5 wt%). A free-standing TiO_2 nanotube layer was obtained, as it can be easily handled with tweezers. TiO_2 nanoparticle viscous paste was spin-coated onto FTO glass substrates, and the free-standing TNT-arrays membranes were transferred onto the paste layers immediately. After being dried in air, the films were sintered at 450°C for 30 min.

2.3. Preparation of the TNT-Arrays/FTO Glass Photoanode. The as-prepared TNT-arrays were transferred onto FTO glass and two drops of 0.1 M Ti-isopropoxide were subsequently added to the TiO_2 nanotube films to form interconnections between the TNT-arrays and the FTO glass. In this work, three kinds of different TiO_2 films (TNT-arrays film, P25 nanoparticle film, and P25/TNT-arrays double-layered composite film) as photoelectrodes were fabricated and their photovoltaic conversion performances were investigated and compared.

2.4. Fabrication Dye-Sensitized Solar Cells. Three kinds of different TiO_2 films were immersed into a 0.3 mM solution of N719 in anhydrous ethanol and kept at room temperature for 24 h. The sensitized electrodes were further sandwiched with the sputtered-Pt FTO glass, separated by a 40 um thick hotmelt spacer. The intervening space was filled with an electrolyte made with 0.3 M LiI, 0.05 M I_2, 0.6 M 1-propyl-3-methylimidazolium iodide, and 0.5 M *tert*-butylpyridine in dry acetonitrile, and the assembled cell was tested immediately. The photographs of the TNT-arrays films at the different stages of the fabrication process are shown in Figure 1.

2.5. Characterization and Measurement. The morphologies of the obtained free-standing TNT-arrays films were characterized using a S-4800 field emission SEM (FESEM, Hitachi, Japan). X-ray diffraction (XRD) patterns were obtained using a D/MAX-IIIC X-ray diffractometer (Akishima-shi, Tokyo, Japan). UV-Vis absorbed spectra of different films were measured by a UV-visible spectrometer (UV2550, Shimadzu, Japan). In order to estimate the dye adsorbed amount on the three kinds of TiO_2 photoelectrodes, we immersed, respectively, the sensitized electrodes into a 0.1 M NaOH solution in a mixed solvent (water : ethanol = 1 : 1, in volume fraction), and afterwards the absorption spectra of the solutions were obtained and the concentration of adsorbed dye was evaluated spectrophotometrically.

The photocurrent-voltage characteristics (J-V curves) of the DSSCs were performed under AM 1.5 G solar simulator (Oriel Sol3A, Newport Corporation, Irvine, CA, USA) at a light intensity of 100 mW cm^{-2}. The electrochemical impedance spectroscopy (EIS) measurements of all the DSSCs were recorded using electrochemical workstation (IM6, Germany) under 100 mW cm^{-2} light illumination condition. The frequency range was explored from 0.1 Hz to 100 kHz, and the applied bias voltage and ac amplitude were set at open-circuit voltage of the DSSCs and 10 mV, respectively.

3. Results and Discussion

3.1. Phase Structures and Morphology. It is well known that the phase structure and crystallinity of TiO_2 are of great influence on its photoelectrochemical properties. Therefore, XRD was used to characterize the changes of phase structures of the prepared TNT-arrays before and after annealing. Figure 2 shows XRD patterns of as-annealed TNT-arrays and annealed TNT-arrays on Ti foil at 450°C, respectively. No peaks were shown in Figure 2(a) because the as-annealed

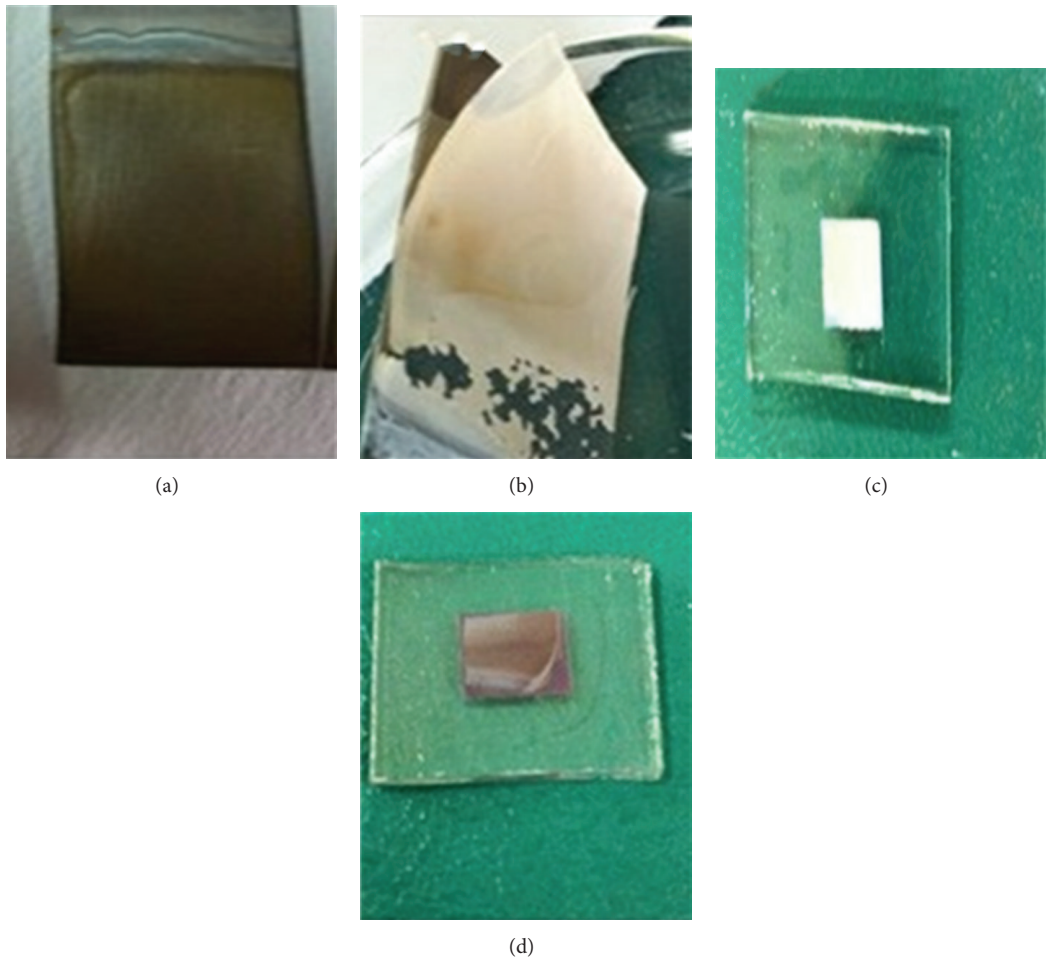

Figure 1: Photographs of TNT-arrays at different fabrication stages: TNT-arrays on the Ti substrate via anodization method (a), TNT-arrays membrane detached from the Ti substrate via a secondary anodization method (b), crystalline TNT-arrays/FTO film after heat treatment before dye loading (c), and N719 dye loaded TNT-arrays/FTO film (d).

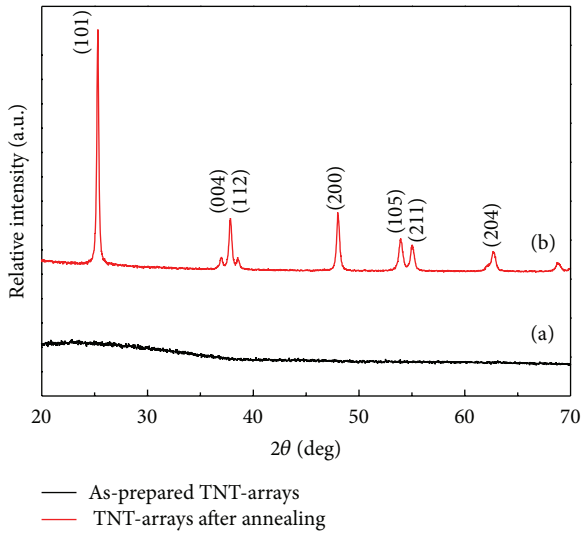

Figure 2: XRD patterns of as-prepared TNT-arrays (a) and TNT-arrays after annealing process at 450°C for 30 min (b).

TNT-arrays have an amorphous structure. However, after annealing process at 450°C for 30 min (as shown in Figure 2(b)), all the diffraction peaks are indexed to the anatase phase of TiO_2, which is consistent with the pure anatase phase of TiO_2 (space group: $I4_1/amd$ (141); JPCDS No. 21-1272).

Figure 3 shows the typical SEM images of TNT-arrays in a top-view, bottom-view, and cross-sectional-view, respectively, which were prepared by anodization of titanium foils at 40 V for 12 h in an ethyl glycol based electrolyte containing NH_4F (0.5 wt%) and deionized water (2 vol%) solution. It can be seen that the closely packed highly ordered nanotube arrays were obtained, which have an average pore diameter of around 120 nm and wall thickness of ca. 20 nm. Figures 3(a) and 3(b) show that the nanotubes opened on the top but closed on the bottom. Figure 3(c) exhibits a cross-sectional SEM image of the TNT-arrays, indicating that the TNT-arrays contain well-aligned nanotubes about 10.7 μm in length which grow vertically from a Ti substrate.

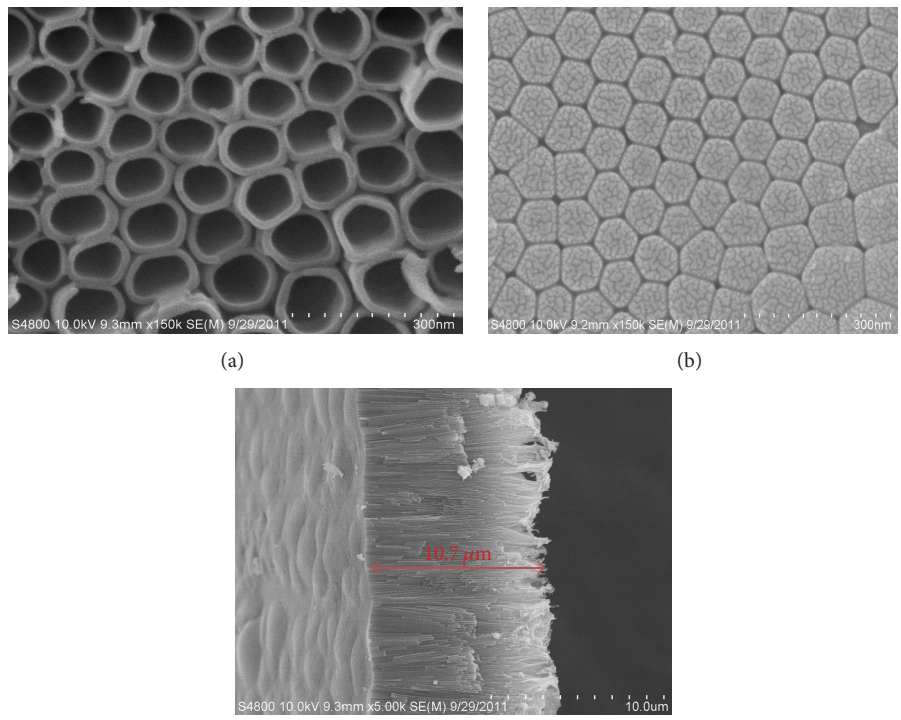

(a) (b)

(c)

Figure 3: SEM images of TNT-arrays in top-view (a), in bottom-view (b), and in cross-sectional-view (c).

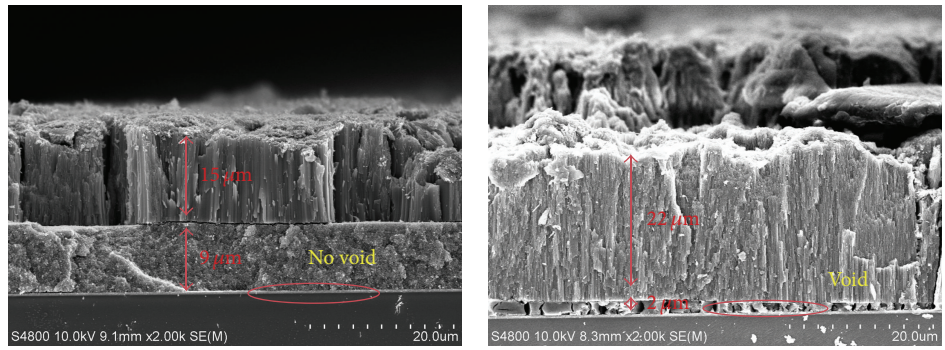

(a) (b)

Figure 4: SEM images of cross-section of double-layer composite film (a) and TNT-arrays film (b).

The cross-sectional SEM images of double-layer film and TNT-arrays film were shown in Figures 4(a) and 4(b). As shown in Figure 4(a), one can clearly recognize the double-layer structure with a 15 μm thick TNT-arrays overlayer and a 9 μm thick TiO_2 nanoparticle underlayer. Compact P25 nanoparticle underlayer will enlarge contact area between the TiO_2 film and FTO glass; meanwhile, it may cut off the direct contact between I_3^- ions and FTO glass. Charge recombination at FTO/TiO_2 interfaces has been prevented and the bonding strength between TiO_2 film and FTO glass has been improved. However, some voids can be seen on the FTO surface in the TNT-arrays film. As shown in Figure 4(b), it cannot cover the FTO surface smoothly in comparison with double-layered film. Consequently, some of I_3^- ions can reach the FTO glass between the interfaces of TNT-arrays film and FTO glass. As a result, the electrons would be back transported from the TNT-arrays photoelectrode to the I_3^- ions.

3.2. UV-Visible Absorbed Spectra and Dye Adsorption Measurements. Figure 5 shows diffuse reflection spectra (DRS) for three photoanodes. The DRS reveals stronger scattering for the pure TNT-arrays films in comparison with that of P25 particle films in the visible and near-infrared region, suggesting better light-scattering capabilities for TNT-arrays films compared with P25 nanoparticles films. The light-scattering capability of the double-layered films is placed in the middle.

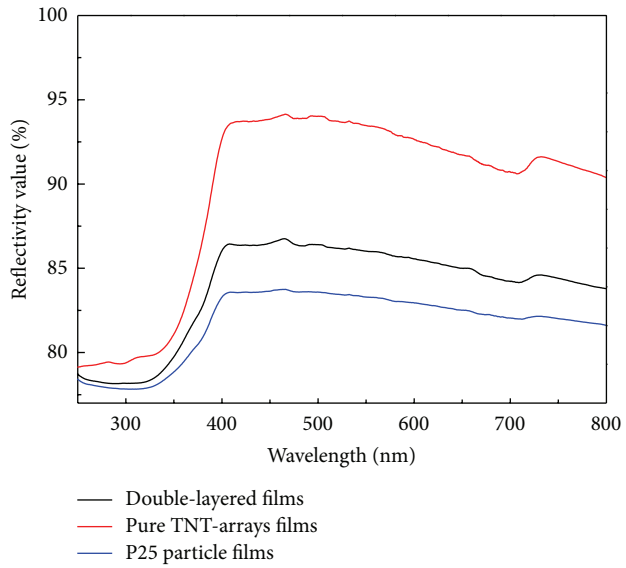

Figure 5: Diffused reflectance spectra of DSSCs based on a nanoparticle film, a TNT-arrays film, and a double-layered film with a similar thickness.

This is because the double-layered film is made of the two different morphological forms of titanium dioxide. The highest light-scattering capability of TNT-arrays is almost attributed to its homogeneous, highly ordered electronic transport paths, in which the incident light can reflect repeatedly to prolong effectively the optical transfer length of photoanode, resulting in enhanced light harvesting efficiency.

The dye adsorption amount in these films is displayed in Table 1. Obviously, the adsorbed amount of dye in double-layered films (4.43×10^{-8} mol cm^{-2}) is slightly higher compared with TNT-arrays (3.54×10^{-8} mol cm^{-2}) or P25 films (3.75×10^{-8} mol cm^{-2}). This is largely attributed to the presence of lots of interfaces between TNT-arrays and particle films in double-layered films, which facilitates the absorption of more amounts of dye molecules in the double-layered films. Meanwhile, it can be seen that both TNT-arrays films and P25 films have almost the same dye adsorption amount. This is because the surface area of TNT-arrays films is the same as that of P25 particle films.

3.3. Photovoltaic Performances of DSSCs. Figure 6(a) shows the dark current-voltage characteristics of DSSCs for three kinds of photoanodes. It is noted that the pure TNT-arrays photoelectrode produces the highest dark current, while the double-layered and P25 photoanode produces the lowest dark current at the same potential of about 0.55 V. These observations reflect a higher recombination at the pure TNT-arrays films than the double-layered films and P25 films. The dark current measurement indicated that the double-layered photoanode had a slower photoelectrons recombination rate, which is more contributed to the photoelectronic performance of DSSCs.

Under illumination, the typical photocurrent density-photovoltage (J-V) curves of the cells made from three kinds of photoanode are shown in Figure 6(b). The detailed photovoltaic parameters are summarized in Table 1. As shown in Table 1, DSSCs based on double-layered film attained a short-circuit current density (J_{sc}) of 15.88 mA cm^{-2} and an open-circuit voltage (V_{oc}) of 0.65 V, leading to a higher PCE of 6.32%. Meanwhile, DSSCs based on pure TNT-arrays film only got a short-circuit current density (J_{sc}) of 12.78 mA cm^{-2}, an open-circuit voltage (V_{oc}) of 0.67 V, and thus a PCE of 5.18%. And then DSSCs based on P25 nanoparticle film only got a short-circuit current density (J_{sc}) of 10.66 mA cm^{-2}, an open-circuit voltage (V_{oc}) of 0.60 V, and thus a lower PCE of 3.65%. Evidently, the PCE of DSSCs based double-layered composite photoanode is 42.4% higher than that of TNT-arrays photoanode, and it is also 49% higher than that of P25 nanoparticle photoelectrode. As a result, the remarkable enhancement of PCE for double-layered photoanode compared to the others is mainly attributed to the improvement of the J_{sc}. The enhanced J_{sc} of the former can be attributed to the lower electronic recombination rate from P25 nanoparticle underlayer and fast electronic transport paths provided by TNT-arrays overlayer. More detailed explanations for the enhancement of η for double-layer TiO_2 photoelectrode will be discussed later.

Table 1: Comparisons of the photovoltaic performances and adsorbed dye amount of DSSCs made from P25 nanoparticle film, TNT-arrays films, and double-layer composite film. All measurements were performed under AM 1.5 one-sun light intensity of mW cm^{-2}, and the thickness of all the films was controlled to be similar (ca. 24 μm).

Photoanode	J_{sc} (mA cm^{-2})	V_{oc} (V)	FF	η (%)	Adsorbed dye amount ($\times 10^{-8}$ mol cm^{-2})
P25 particle	10.66	0.60	0.64	3.65	3.75
TNT-arrays	12.78	0.67	0.52	5.18	3.54
Double-layer	15.88	0.65	0.61	6.32	4.43

3.4. EIS Analyses. The electrochemical impedance spectroscopy (EIS) analysis of DSSCs fabricated with the three different TiO_2 photoanodes noted above was performed to elucidate the characteristics of electron transport in the DSSCs. The EIS measurements were carried out at the frequency range of 10^{-1}–10^5 Hz at V_{oc} under one-sun illumination to determine impedance of solar cells. The Nyquist plots and the equivalent circuit diagram are shown in Figure 7(a) and in the inset of Figure 7(a). According to the EIS model for TiO_2 reported in our previous work [23], the Nyquist plots exhibit a large semicircle at low frequencies and a small one at high frequencies. The smaller semicircle in the high frequency represents the redox charge transfer at the counter electrode and the larger semicircle in the low frequency denotes the electron transfer at the TiO_2-dye-electrolyte interface, which were fitted as R_{ct} and R_w using Z-view software, whereas R_s represents the sheet resistance of FTO and the contact resistance between the FTO and TiO_2 film. The R_s, R_{ct}, and R_w data are collected in Table 2. Obviously, the TNT-arrays films show

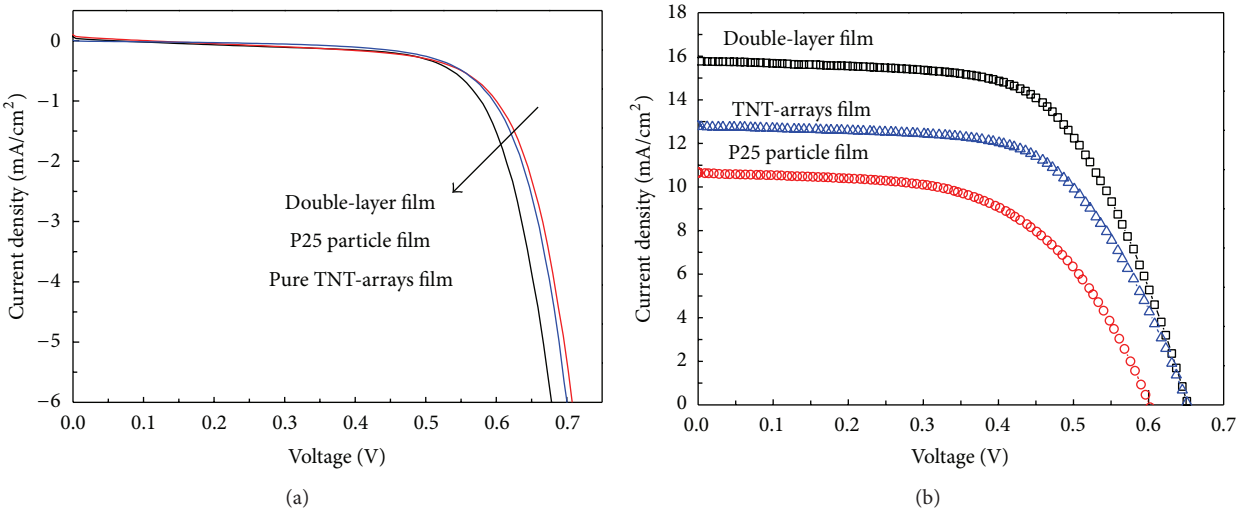

FIGURE 6: *I-V* performance of the DSSCs based on P25 nanoparticle film, TNT-arrays films, and double-layer composite film in the dark (a) and under AM 1.5 illuminations (b).

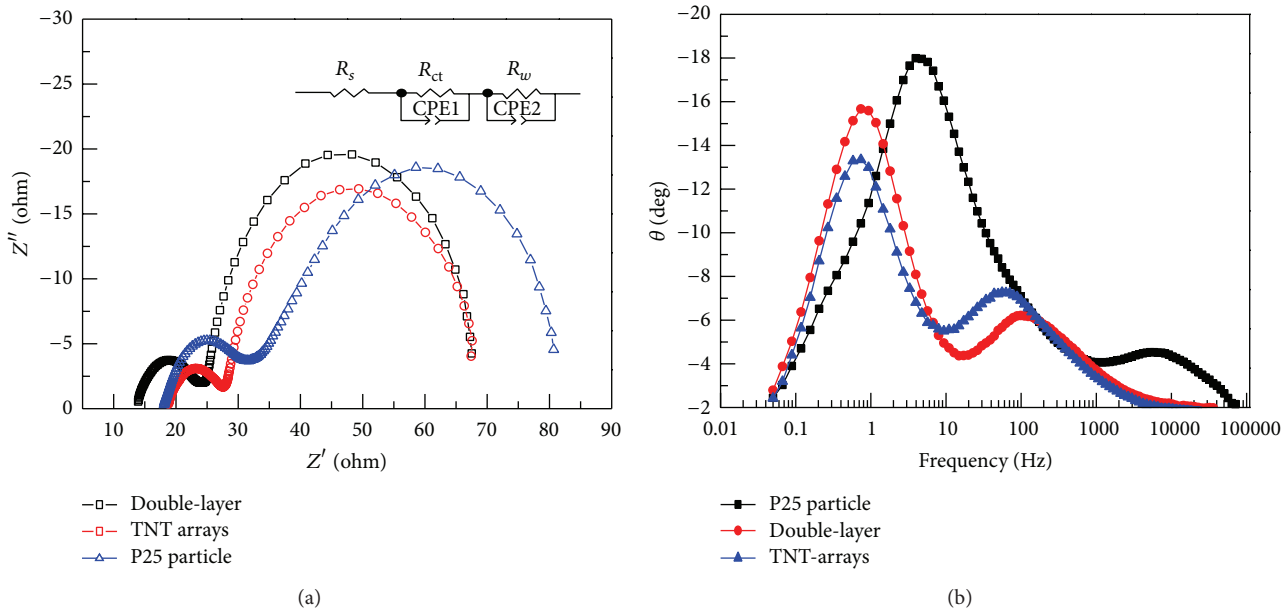

FIGURE 7: EIS spectra of DSSCs based on double-layer composite film, TNT-arrays film, and P25 nanoparticle film. (a) Nyquist plots and (b) Bode phase plots.

the lowest values for R_{ct} and R_w resistance among three cells, suggesting that more efficient charge-transfer process at the Pt counter electrode/redox electrolyte interface and the dye-coated TNT-arrays/electrolyte interface occurs. However, the TNT-arrays films also display the poor contact between TNT-arrays films and FTO conducting glass due to the highest value of R_s resistance. Therefore, the double-layered films possess the lowest value of R_s and slightly lower values for R_{ct} and R_w resistance, resulting in the optimal conversion efficiency among the three cells, which corresponds well with the aforementioned *J-V* characterization data. The Bode phase plots (Figure 7(b)) of EIS spectra display the frequency peaks of the charge-transfer process at different interfaces for three kinds of cells. The electron lifetime (τ_e) in DSSCs can be calculated from the maximum frequency of the low-frequency peak (f_{max}) value following the equation $\tau_e = 1/2\pi f_{max}$ [24]. As is shown in Table 2, both TNT-arrays films and the double-layered films indicate the relatively longer electron lifetime compared to P25 nanoparticle films. Hence the decrease in the transport resistance and increase in electronic lifetime are observed in the double-layered films. Especially, it is worth noting that the value for the R_s is almost a critical role for PCE for solar cells, which means that better electronic contact between TiO_2 film and FTO conducting glass is very important for DSSCs, leading to the enhancement of power conversion efficiency.

Table 2: Parameters obtained by fitting the impedance spectra of DSSCs using the equivalent circuit in Figure 6.

Sample	R_s (Ω)	R_{ct} (Ω)	R_w (Ω)	τ (ms)
P25 particle	17.84	15.84	59.86	42.2
TNT-arrays	18.33	10.21	43.38	60.1
Double-layer	12.33	12.38	46.42	59.5

4. Conclusions

In conclusion, we successfully fabricated a TiO_2 double-layer composite film consisting of hierarchical TNT-arrays as overlayer and P25 nanoparticles as underlayer for applications as improved dye-sensitized solar cells. The XRD patterns of the double-layered films are indexed to the excellent anatase phase of TiO_2. The microscopy technique confirms the TNT-arrays structure is highly ordered and vertically aligned on the substrate, which offers effective transport paths for electron. DSSCs based on the double-layered films exhibit 6.32% power conversion efficiency (PCE), which is 73% higher than that of P25 nanoparticle films (3.65%) and 22% higher than that of TNT-arrays films (5.18%) under similar film thickness (ca. 24 μm) at a constant irradiation of 100 mW cm^{-2}. The enhanced PCE of DSSCs based double-layered films is attributed to the good contact with FTO, fast electron transport, superior light-scattering ability and slower charge recombination. Thus, the double-layered films applied in DSSCs open up a new route to fabricate the low-cost, environmentally safe, and improved solar-to-electric efficiency.

Conflict of Interests

The authors declare that there is no conflict of interests regarding the publication of this paper.

Acknowledgments

This work was supported by the NSFC (51102087, 11172221, and 11205066) and the Fundamental Research Funds for the Central Universities (WUT: 2014-Ia-028). This work was also financially supported by the Ph.D. Programs Foundation of Ministry of Education of China (20114208110004) and Wuhan Science and Technology Bureau of Hubei Province of China (201051730551 and 2013010501010143).

References

[1] B. O. 'Regan and M. Grazel, "A low-cost, high-efficiency solar cell based on dye-sensitized colloidal TiO_2 films," *Nature*, vol. 353, pp. 737–740, 1991.

[2] A. Yella, H. W. Lee, H. N. Tsao et al., "Porphyrin-sensitized solar cells with cobalt (II/III)-based redox electrolyte exceed 12 percent efficiency," *Science*, vol. 334, no. 6056, pp. 629–634, 2011.

[3] X. Feng, K. Shankar, O. K. Varghese, M. Paulose, T. J. Latempa, and C. A. Grimes, "Vertically aligned single crystal TiO_2 nanowire arrays grown directly on transparent conducting oxide coated glass: synthesis details and applications," *Nano Letters*, vol. 8, no. 11, pp. 3781–3786, 2008.

[4] H. S. Kim, Y. J. Kim, W. Lee, and S. H. Kang, "One-pot synthesis of peacock-shaped TiO_2 light scattering layer with TiO_2 nanorods film for dye-sensitized solar cells," *Applied Surface Science*, vol. 273, pp. 226–232, 2013.

[5] A. S. Nair, R. Jose, Y. Shengyuan, and S. Ramakrishna, "A simple recipe for an efficient TiO_2 nanofiber-based dye-sensitized solar cell," *Journal of Colloid and Interface Science*, vol. 353, no. 1, pp. 39–45, 2011.

[6] K. Zhu, N. R. Neale, A. Miedaner, and A. J. Frank, "Enhanced charge-collection efficiencies and light scattering in dye-sensitized solar cells using oriented TiO_2 nanotubes arrays," *Nano Letters*, vol. 7, no. 1, pp. 69–74, 2007.

[7] S. P. Albu, A. Ghicov, J. M. Macak, R. Hahn, and P. Schmuki, "Self-organized, free-standing TiO_2 nanotube membrane for flow-through photocatalytic applications," *Nano Letters*, vol. 7, no. 5, pp. 1286–1289, 2007.

[8] T. Maiyalagan, B. Viswanathan, and U. V. Varadaraju, "Fabrication and characterization of uniform TiO_2 nanotube arrays by sol-gel template method," *Bulletin of Materials Science*, vol. 29, no. 7, pp. 705–708, 2006.

[9] T. S. Kang, A. P. Smith, B. E. Taylor, and M. F. Durstock, "Fabrication of highly-ordered TiO_2 nanotube arrays and their use in dye-sensitized solar cells," *Nano Letters*, vol. 9, no. 2, pp. 601–606, 2009.

[10] K. P. Yu, W. Y. Yu, M. C. Kuo, Y. C. Liou, and S. H. Chien, "Pt/titania-nanotube: a potential catalyst for CO_2 adsorption and hydrogenation," *Applied Catalysis B: Environmental*, vol. 84, no. 1-2, pp. 112–118, 2008.

[11] S. Sreekantan and L. C. Wei, "Study on the formation and photocatalytic activity of titanate nanotubes synthesized via hydrothermal method," *Journal of Alloys and Compounds*, vol. 490, no. 1-2, pp. 436–442, 2010.

[12] C. T. Hsieh, M. H. Lai, and C. Pan, "Synthesis and visible-light-derived photocatalysis of titania nanosphere stacking layers prepared by chemical vapor deposition," *Journal of Chemical Technology and Biotechnology*, vol. 85, no. 8, pp. 1168–1174, 2010.

[13] D. Gong, C. A. Grimes, O. K. Varghese et al., "Titanium oxide nanotube arrays prepared by anodic oxidation," *Journal of Materials Research*, vol. 16, no. 12, pp. 3331–3334, 2001.

[14] J. M. Macak and P. Schmuki, "Anodic growth of self-organized anodic TiO_2 nanotubes in viscous electrolytes," *Electrochimica Acta*, vol. 52, no. 3, pp. 1258–1264, 2006.

[15] S. Sreekantan, R. Hazan, and Z. Lockman, "Photoactivity of anatase-rutile TiO_2 nanotubes formed by anodization method," *Thin Solid Films*, vol. 518, no. 1, pp. 16–21, 2009.

[16] A. El Ruby Mohamed and S. Rohani, "Synthesis of titania nanotube arrays by anodization," *AIDIC Conference Series*, vol. 9, pp. 121–129, 2009.

[17] A. El Ruby Mohamed and S. Rohani, "Modified TiO_2 nanotube arrays (TNTAs): progressive strategies towards visible light responsive photoanode, a review," *Energy and Environmental Science*, vol. 4, no. 4, pp. 1065–1086, 2011.

[18] D. Kuang, J. Brillet, P. Chen et al., "Application of highly ordered TiO_2 nanotube arrays in flexible dye-sensitized solar cells," *ACS Nano*, vol. 2, no. 6, pp. 1113–1116, 2008.

[19] C. J. Lin, W. Y. Yu, and S. H. Chien, "Rough conical-shaped TiO_2-nanotube arrays for flexible backilluminated dye-sensitized solar cells," *Applied Physics Letters*, vol. 93, Article ID 133107, 2008.

[20] P. T. Hsiao, Y. J. Liou, and H. Teng, "Electron transport patterns in TiO_2 nanotube arrays based dye-sensitized solar cells under frontside and backside illuminations," *Journal of Physical Chemistry C*, vol. 115, no. 30, pp. 15018–15024, 2011.

[21] G. K. Mor, K. Shankar, M. Paulose, O. K. Varghese, and C. A. Grimes, "Use of highly-ordered TiO_2 nanotube arrays in dye-sensitized solar cells," *Nano Letters*, vol. 6, no. 2, pp. 215–218, 2006.

[22] J. Hyeoká Park and M. GuáKang, "Employment information," *Chemical Communications*, vol. 25, no. 39, pp. 2867–2869, 2008.

[23] G. Dai, L. Zhao, S. Wang et al., "Double-layer composite film based on sponge-like TiO_2 and P25 as photoelectrode for enhanced efficiency in dye-sensitized solar cells," *Journal of Alloys and Compounds*, vol. 539, pp. 264–270, 2012.

[24] S. M. Park and J. S. Yoo, "Peer reviewed: electrochemical impedance spectroscopy for better electrochemical measurements," *Analytica Chemistry*, vol. 75, no. 21, pp. 455–461, 2003.